

# All-in-One: Validation and Versatile Applications of a Novel Chemical Ionization Mass Spectrometer for Simultaneous Measurements of Volatile Organic and Inorganic Compounds

Yunhua Chang,<sup>1,\*</sup> Tianhao Ding,<sup>1</sup> Haifeng Yu,<sup>1</sup> Yuanjian Yang,<sup>1</sup> Liang Zhu,<sup>2</sup> Xiaozheng Liu,<sup>2</sup> and Wen Tan<sup>2,\*</sup>

<sup>1</sup>State Key Laboratory of Climate System Prediction and Risk Management, Center for Atmospheric Chemistry and Isotope Research, Nanjing University of Information Science & Technology, Nanjing 210044, P. R. China

<sup>2</sup>Tofwerk China, Nanjing, 411800, P. R. China

*Correspondence to:* Yunhua Chang (changy13@nuist.edu.cn) and Wen Tan (wen.tan@tofwerk.com)

**Abstract.** Volatile organic compounds (VOCs) and volatile inorganic compounds (VICs) are crucial players in atmospheric chemistry, and their coexistence in industrial environments, particularly semiconductor manufacturing, presents significant obstacles to production yields. The simultaneous and high-time-resolution measurements of both VOCs and VICs from a single platform have long been an analytical Achilles' heel, often requiring compromises in sensitivity or selectivity for certain compound classes. This study introduces and comprehensively evaluates a novel Vocus B Chemical Ionization Time-of-Flight Mass Spectrometer (CI-TOF-MS), an improved "all-in-one" solution that overcomes this challenge by rapidly switching between reagent ions and polarities. Laboratory-based calibrations for a suite of VOCs and VICs, including ammonia (NH<sub>3</sub>) and various amines, demonstrated excellent linearity ( $R^2 > 0.99$ ) and high sensitivity. An inter-comparison experiment for NH<sub>3</sub> with an established cavity ring-down spectroscopy analyzer (Picarro G2103) showed strong overall agreement in tracking major pollution events and diurnal trends. We demonstrate the instrument's versatility through three distinct applications: (1) stationary *in-situ* monitoring in urban Nanjing, which captured complex pollution dynamics and identified a previously overlooked industrial solvent hotspot; (2) mobile laboratory deployment along the Nanjing-Hefei corridor, which successfully mapped pollution gradients and attributed sources in real-time; and (3) real-time monitoring of Airborne Molecular Contaminants from a Front Opening Unified Pod, simulating its utility for yield improvement in semiconductor fabrication. This work establishes the Vocus B as a versatile tool, offering a unified and efficient approach to elucidate the complex chemical interactions in both atmospheric science and industrial process control.

## 1 Introduction

Volatile organic compounds (VOCs) and volatile inorganic compounds (VICs) are fundamental constituents of the Earth's atmosphere, originating from a vast range of natural and anthropogenic sources (Park et al., 2013; McDonald Brian et al., 2018; Gu et al., 2021; Van Damme et al., 2018; Ehn et al., 2014). VOCs encompass a diverse group of carbon-based chemicals (Mohr et al., 2019), while VICs include key acidic gases (sulfur dioxide or SO<sub>2</sub>, nitrogen oxides or NO<sub>x</sub>) and the principal

atmospheric base, ammonia (NH<sub>3</sub>) (Wang et al., 2020b). Their chemical transformations are intrinsically linked to major environmental issues, with impacts arising from tightly coupled chemical interactions (Nie et al., 2022; Yao et al., 2018). For instance, ozone formation is driven by a NO<sub>x</sub>-catalyzed cycle, where both VOCs and NO<sub>x</sub> can be co-limiting reactants (Seinfeld and Pandis, 2012; Pye et al., 2019). This complexity also manifests in urban odor pollution, a major public nuisance often caused by a complex mixture of VICs like NH<sub>3</sub> and diverse VOCs (e.g., sulfides and other nitrogenous compounds) (Chang et al., 2021; Yuan et al., 2017b). In this context, mobile, real-time measurements are critical for applications like fenceline monitoring to pinpoint industrial emission sources and protect communities (Zhang et al., 2024; Chang et al., 2022). Because these atmospheric systems are deeply intertwined, a comprehensive understanding and effective management of air quality hinges on the concurrent, high-resolution measurement of both VOC and VIC species.

This analytical imperative extends with arguably even greater urgency to high-precision manufacturing. In the semiconductor industry, the same co-presence of VOCs and VICs manifests as Airborne Molecular Contamination (AMC), degrading production yields and device reliability through a cascade of failure pathways (Den et al., 2020; Mansouri et al., 2023). AMCs are broadly classified into molecular acids (MAs), bases (MBs), condensable organics (MCs), and dopants (MDs). Each class presents a unique threat: the direct deposition of MCs and MBs creates detrimental surface films and causes haze on critical photolithography optics; acidic MAs aggressively corrode metallic interconnects; and MDs-airborne compounds containing elements like boron or phosphorus-cause uncontrolled shifts in transistor electrical properties. A particularly insidious threat arises from the *in-situ* reaction between MAs and MBs, which generates nano-scale salt particles that deposit as ‘killer defects’ (Kirkby et al., 2011). This multifaceted threat intensifies dramatically as manufacturing nodes evolve to the sub-10 nm scale, where the process becomes critically sensitive to even parts-per-trillion in volume (pptv) concentrations (Chen et al., 2022).

The simultaneous detection of both VOCs and VICs with a single instrument has remained an important analytical goal for atmospheric scientists and industrial process engineers alike (Lee et al., 2014; Yang et al., 2022; Tiszenkel et al., 2024; Riva et al., 2024; Huang et al., 2009; Reinecke et al., 2023). Recently, while Chemical Ionization Mass Spectrometry (CIMS) has enabled the detection of both VOCs and key VICs, such as ammonia and amines, using techniques like iodide-adduct or ethanol-based ionization (You et al., 2014; Tiszenkel et al., 2024; Pfeifer et al., 2020; Zheng et al., 2015), optimizing the concurrent measurement of chemically disparate species still presents significant challenges (Yuan et al., 2017a; Hanson et al., 2011). For instance, widely-used platforms like the Proton-Transfer-Reaction Mass Spectrometer (PTR-MS) are highly effective for a broad range of organics but can exhibit lower sensitivity or require alternative reagent ions for the quantification of key VICs like NH<sub>3</sub> (Norman et al., 2007; Link et al., 2025). Conversely, other ionization schemes, such as those using iodide adducts, are excellent for inorganic acids but are not suited for many non-polar VOCs (You et al., 2014; Vera et al., 2022).

Consequently, a comprehensive assessment has historically demanded a patchwork of separate technologies—such as optical techniques like Cavity Ring-Down Spectroscopy (CRDS) for NH<sub>3</sub> (Chang et al., 2021)—or the use of a single CIMS instrument under fixed conditions that represent a compromise in performance for some of the target analytes. This reliance on a multi-

instrument suite or sub-optimal configurations increases operational cost, logistical complexity, and can introduce scientific uncertainty from separate sampling inlets and complex data synchronization. To overcome the need for such analytical compromises, here we introduce the Vocus B Chemical Ionization Time-of-Flight Mass Spectrometer (CI-TOF-MS), a novel instrument. Unlike specialized analyzers (e.g., CRDS) that offer benchmark precision but are limited to single species, the Vocus B is engineered to provide a unified “all-in-one” solution. This platform consolidates the capabilities of multiple separate analyzers by measuring both VOCs and VICs simultaneously with sub-second switching between optimized reagent ions. This significantly reduces the instrumental footprint and operational complexity while preserving the temporal correlation between chemically diverse species. Herein, we present a comprehensive evaluation of its performance, first detailing its laboratory validation through calibrations and inter-comparisons. We then demonstrate its unique versatility across three distinct and challenging scenarios: stationary urban atmospheric monitoring, mobile regional pollution mapping, and targeted real-time industrial process simulation.

## 2. Materials and methods

**2.1 The Vocus B CI-TOF Mass Spectrometer.** The Vocus B CI-TOF-MS (hereafter referred to as Vocus B; ToFwerk AG, Thun, Switzerland) represents a recent development in Chemical Ionization Time-of-Flight Mass Spectrometry, a technique widely applied in instruments like the PTR-MS. The design of the Vocus B is centered around the novel Vocus Adduct Ionization Mechanism (AIM) reactor, a conical ion-molecule reactor operating at a medium pressure of approximately 50 mbar. This configuration is engineered to enhance measurement sensitivity and stability by promoting the formation of adduct ions while minimizing the fragmentation of parent molecules, simplifying mass spectral interpretation. Crucially, the conical shape and conductive polytetrafluoroethylene (PTFE) construction of the AIM reactor are designed to reduce analyte-wall interactions, leading to a faster time response and minimized memory effects for polar, sticky compounds like amines.

The foundational design, operational principles, and technical characterization of the AIM reactor have been comprehensively presented in a complementary study recently (Riva et al., 2024). That work provides a detailed evaluation of the reactor’s core functionalities and establishes its fundamental performance benchmarks, reporting exceptionally low 1-min limits of detection (LODs) across various ionization schemes for key species, such as 1.0 pptv for  $\text{NH}_3$  and 1.4 pptv for  $\alpha$ -pinene. Building directly upon that foundational instrument science, the present study focuses on a comprehensive validation of the instrument’s quantitative performance and demonstrating its utility and robustness as a field-deployable tool for the complex real-world applications detailed herein.

A defining feature of the Vocus B is the capacity for rapid, seamless switching of both reagent ions and polarity. The instrument is equipped with multiple vacuum ultraviolet ion sources that operate by photoionizing a precursor gas (e.g., acetone or benzene) to initiate the ion-molecule reactions that produce the desired reagent ions. This system allows for switching between different ionization schemes on a millisecond timescale, enabling the quasi-simultaneous measurement of chemically diverse compound

classes from a single instrument. Furthermore, the instrument can switch between positive and negative ion detection modes  
95 in under 500 ms, providing a holistic chemical characterization of complex gas mixtures. In the field campaigns presented  
here, we typically employed a cycle where the instrument dwelt in each mode for approximately 500 ms to 1 second, resulting  
in a total cycle time (and data resolution) of approximately 2 seconds (0.5 Hz) for the full suite of measurements. For this  
study, the following ionization modes were primarily utilized:

Protonated Acetone Mode: Generated by introducing acetone into the ion source, this mode is particularly effective for  
100 detecting  $\text{NH}_3$  and various amine compounds through the formation of protonated acetone-analyte clusters.

Benzene Mode: Using benzene as the reagent gas, this mode is ideal for the detection of a wide range of VOCs, including  
aromatic hydrocarbons and other less polar species, via charge transfer reactions.

Iodide Mode: In this negative ion mode, iodide ions ( $\text{I}^-$ ) are used as reagent ions to detect acidic and highly oxygenated  
compounds through adduct formation. This mode is highly sensitive to species like inorganic acids (e.g.,  $\text{HCl}$ ,  $\text{HNO}_3$ ) and  
105 oxygenated VOCs.

The ions generated in the AIM reactor are guided through a series of ion optics, including a quadrupole ion guide, into a high-  
resolution time-of-flight (TOF) mass analyzer. For the operational settings in this study, a mass resolving power ( $m/\Delta m$ ) of  
 $\sim 1500$  was consistently achieved. While higher resolutions are available, this setting provided an optimal balance between  
sensitivity and the ability to resolve key isobaric interferences relevant to this work.

110 **2.2. Experimental Setup and Validation.** The quantitative performance of the Vocus B was validated through extensive  
laboratory calibrations using multiple ionization modes. For compounds available as certified gas standards (e.g.,  $\text{NH}_3$ ,  
aromatics), multi-point calibrations were performed by dynamically diluting the standards with high-purity nitrogen to  
generate concentration gradients representative of typical ambient conditions (e.g., up to 40 ppb for  $\text{NH}_3$ , up to 20 ppb for  
amines and other VOCs) (De Gouw and Warneke, 2007). For reactive species not available in gas cylinders, such as aliphatic  
115 amines, a liquid calibration system was employed. Standard aqueous solutions were nebulized into a heated carrier gas flow,  
generating a stable and quantifiable gas-phase concentration for calibration (Isaacman et al., 2011). For all analytes, the  
instrument response was plotted against known concentrations to generate calibration curves, determine sensitivities  
(cps/ppbv), and assess linearity.

To rigorously evaluate the Vocus B under dynamic, real-world conditions, an *in-situ* inter-comparison was conducted during  
120 an intensive multi-day campaign in September 2025. The instrument was co-located with a Picarro G2103 ammonia analyzer,  
a widely recognized benchmark for its high precision and accuracy in measuring atmospheric  $\text{NH}_3$  (Chang et al., 2021). The  
CRDS technique achieves its exceptional sensitivity and molecular specificity by measuring the absorption of light over a km-  
scale effective pathlength within a high-finesse optical cavity. Both instruments sampled ambient air through a common, heated

perfluoroalkoxy inlet to eliminate sampling discrepancies. The objective of this experiment was not merely to validate, but to  
125 critically assess the performance differences between the two advanced platforms, particularly their ability to resolve the fine-  
scale temporal structures of pollution events. Data from the Picarro G2103 were recorded at a 1 Hz frequency, while the Vocus  
B operated at a 0.5 Hz data acquisition rate, cycling through its ionization modes. For direct comparison, the relevant NH<sub>3</sub> data  
points from the Vocus B were time-aligned with the CRDS dataset for linear regression and time-series analysis.

**2.3. Field Deployments.** Following laboratory validation, the Vocus B was deployed for a stationary, in-situ atmospheric  
130 monitoring campaign from November to December 2024 at an urban site in Nanjing Pukou R&D Park, with the inlet situated  
on the 15th floor of an office building. The instrument was operated continuously at a 0.5 Hz data acquisition rate, cycling  
through its multiple ionization modes to provide a comprehensive chemical characterization of the urban atmosphere. This  
deployment was designed to test the instrument's long-term stability and robustness under variable meteorological conditions  
and fluctuating pollution levels. A key objective was to demonstrate its "all-in-one" ability to simultaneously capture the  
135 dynamic changes and diurnal profiles of a diverse suite of co-existing pollutants, providing a holistic view of urban atmospheric  
chemistry.

Subsequently, the Vocus B was integrated into a mobile laboratory for a regional measurement campaign conducted in June  
2025. The mobile platform was equipped with an independent power supply and a dedicated, forward-facing, low-residence-  
time sampling inlet designed to minimize exhaust self-sampling and ensure a rapid response to changing ambient conditions.  
140 The platform was driven along the approximately 170 km corridor between Nanjing and Hefei, traversing a complex and  
representative landscape of suburban corridors, industrial zones, and extensive agricultural areas. This mobile deployment  
provided an ideal test case for leveraging the instrument's "all-in-one" capability for spatial mapping and real-time source  
identification by pinpointing the unique chemical fingerprints of different emission sectors.

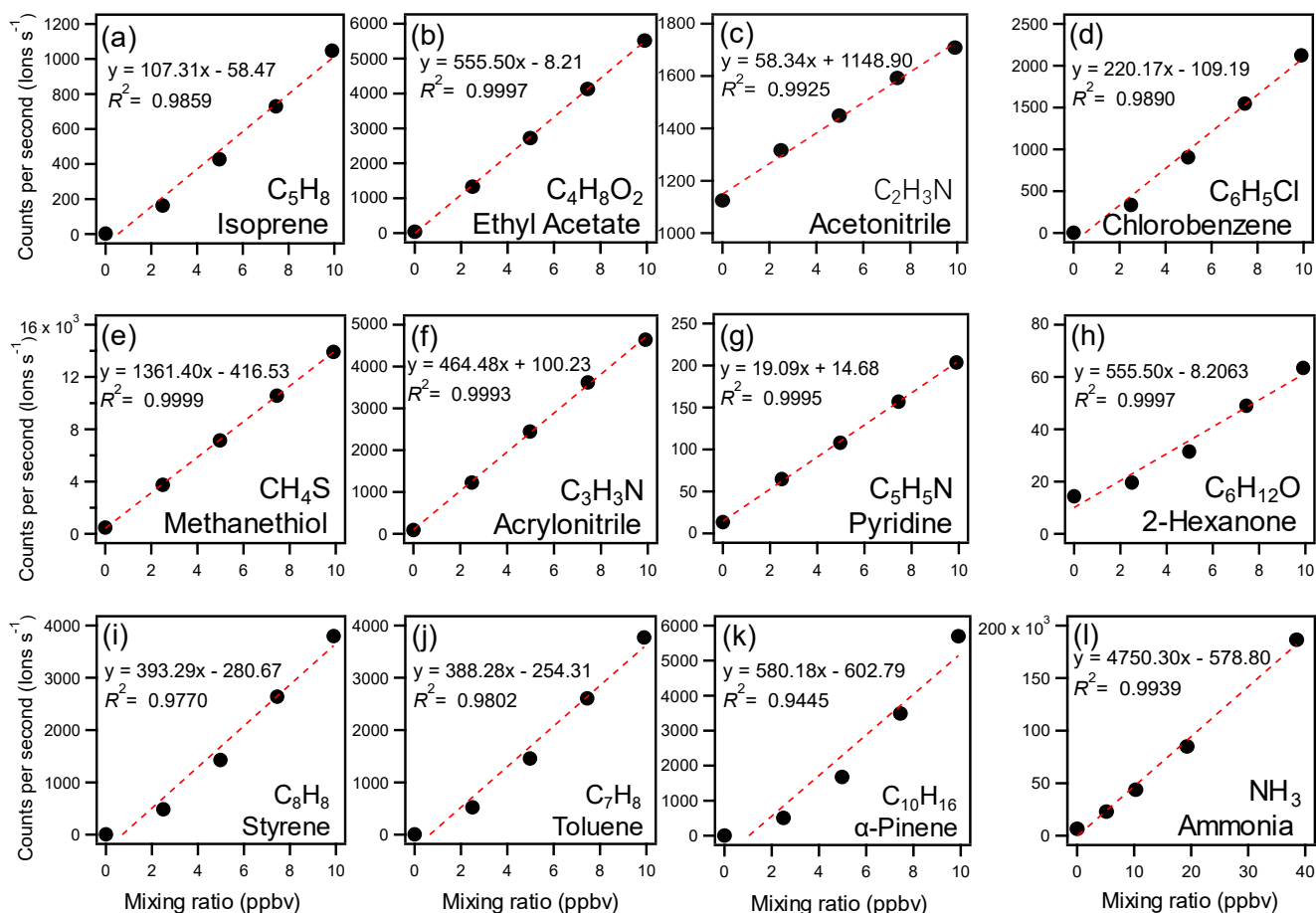
The third application addressed a critical challenge in industrial process control. In this context, the Front Opening Unified  
145 Pod (FOUP) is a critical carrier for wafer transport and storage in semiconductor manufacturing, where its internal cleanliness  
has a direct influence on wafer yield. While mitigating particulate contamination is crucial, controlling AMC within FOUPs  
is of paramount importance. The polymeric materials used in FOUP construction (e.g., polypropylene, PP; polycarbonate, PC)  
behave like molecular sponges, continuously adsorbing and retaining trace gas species from the surrounding environment.  
When FOUPs are introduced into cleaner environments, these adsorbed contaminants can desorb and critically impact device  
150 performance. To demonstrate the utility of Vocus B for managing this threat, a controlled laboratory experiment was conducted  
on July 1, 2025, to simulate a real-time FOUP cleaning validation. A standard FOUP (approx. 50 L) was continuously purged  
with high-purity nitrogen (N<sub>2</sub>) at 5 L min<sup>-1</sup>. After establishing a clean background, a liquid solution containing a mixture of  
typical AMCs (including NH<sub>3</sub>, toluene, hydrogen fluoride or HF, hydrogen chloride or HCl, and SO<sub>2</sub>) was injected to simulate  
a contamination event. The instrument then monitored the decay of these contaminants with a 2-s time resolution to  
155 characterize the outgassing dynamics during the purge cycle.

### 3. Results and discussion

**3.1. Laboratory Performance Evaluation.** A primary objective of the laboratory evaluation was to establish the sensitivity and linearity of the Vocus B for a range of common VOCs. Using a certified gas standard, five-point calibrations were performed with the benzene reagent ion mode, which is highly effective for a broad range of organics via charge transfer.

160 Figure 1a-1k presents the calibration curves for eight representative compounds spanning multiple chemical classes, including a biogenic diene (isoprene), an ester (ethyl acetate), a ketone (2-hexanone), and various aromatics (chlorobenzene, styrene, etc.). All tested compounds displayed excellent linearity ( $R^2 \geq 0.99$ ) across a concentration range of 0-10 ppbv. Notably, the instrument demonstrated high sensitivities (in counts per second per ppbv, cps/ppbv) for all species, particularly for the aromatic compounds, which is consistent with the expected high efficiency of charge transfer reactions for these molecules.

165 This comprehensive result confirms the Vocus B is a reliable and robust tool for the accurate quantification of standard VOCs, providing a strong foundation for its application in complex environments. Calibration results for additional VOCs and representative mass spectra of three reagents are provided in Supplementary Figure S1 and S2, respectively.



170 **Figure 1.** Laboratory calibration curves for (a-k) representative VOCs from a certified gas standard and (l) the key inorganic compound, NH<sub>3</sub>. The VOCs were calibrated using the benzene reagent ion mode, while NH<sub>3</sub> was calibrated using the protonated acetone mode.

The evaluation of VICs in this study focused on NH<sub>3</sub> as a primary target due to its dual role as the most abundant atmospheric base (Yan et al., 2024; Gu et al., 2022) and a critical MB contaminant in industrial cleanrooms (Den et al., 2006). The calibration for NH<sub>3</sub>, also conducted in the protonated acetone mode, yielded outstanding results (Figure 1l). The response was highly linear (R<sup>2</sup> = 0.99) over a wide and environmentally relevant concentration range of 0-40 ppbv. The instrument demonstrated an exceptionally high sensitivity of approximately 4750 cps/ppbv, a value that enables robust ultra-trace detection at the single-digit pptv level. While the Vocus B is also designed to measure acidic VICs like HCl and HNO<sub>3</sub> using its iodide ionization mode, this study prioritized the validation of NH<sub>3</sub> because of its critical relevance and the significant technical challenges associated with generating stable, low-concentration standards for highly corrosive acidic gases. The

excellent performance for  $\text{NH}_3$  therefore serves as a strong proof-of-concept for the overall VIC measurement capabilities of the Vocus B.

Beyond standard VOCs, a key objective of this work is the detailed characterization of the instrument response for amines. While typically present at concentrations 2-3 orders of magnitude lower than  $\text{NH}_3$ , amines are disproportionately important in the atmosphere in terms of initiating new particle formation and triggering urban odor issues (Almeida et al., 2013; Yao et al., 2016; Murphy et al., 2007). However, their high reactivity and surface stickiness make them exceptionally challenging to measure and largely hinder the availability of commercial gas standards (Zheng et al., 2015; Vandenboer et al., 2011). To overcome this, we utilized a liquid calibration system, as described in the methods section. A key mechanistic feature of the employed protonated acetone mode is the detection of both the protonated ion ( $[\text{M}+\text{H}]^+$ ) and the protonated acetone adduct ( $[\text{M}+\text{C}_3\text{H}_6\text{O}\cdot\text{H}]^+$ ); the total sensitivity is the sum of these two signals. As shown in Figure 2, our four-point calibrations for six common amines (methylamine, ethylamine, dimethylamine, diethylamine, trimethylamine, and triethylamine) all exhibited excellent linearity ( $R^2 > 0.98$ ), validating the quantitative capability of the Vocus B for these crucial compounds. This high performance for notoriously difficult-to-measure species underscores the effectiveness of the Vocus AIM reactor design in minimizing inlet losses and memory effects, highlighting the immense potential of this “all-in-one” platform to address long-standing analytical challenges in measuring amines.

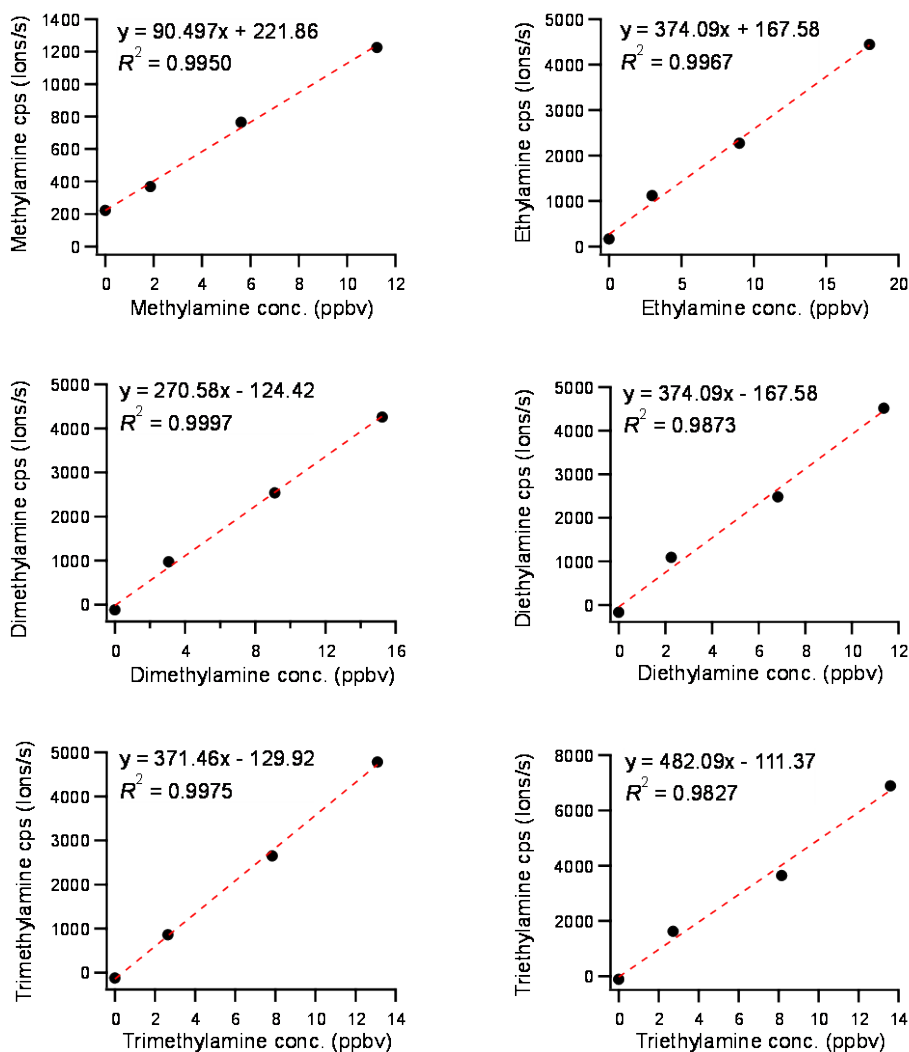


**Figure 2.** Laboratory four-point calibration curves for six common aliphatic amines generated from liquid standards. All calibrations were performed in the protonated acetone mode.

In the measurement of ambient amines, however, another well-known analytical challenge is the prevalence of isobaric isomers, which is an inherent limitation of mass spectrometry without prior chromatographic separation (Sullivan et al., 2020; Place et al., 2017). A classic example is ethylamine and dimethylamine, which are both detected as the  $C_2H_8N^+$  ion and are thus inseparable by the Vocus B. A contribution of this work is that, unlike many previous studies that relied on a single sensitivity factor, we have provided distinct, experimentally-determined sensitivities for each individual isomer. This allows for a more accurate quantification of the total isomer sum concentration, which can be reported, for example, as “C2-amines”. When reporting the sum as “C2-amines” for ambient data, we apply an average sensitivity factor derived from the two isomers. While

this introduces a degree of uncertainty (approximately  $\pm 20\text{-}30\%$  based on the slope difference) depending on the actual mixing ratio of the isomers in the air, it provides a “best estimate” total concentration. This approach improves quantification over previous studies that might arbitrarily apply the sensitivity of just one isomer to the total signal. This standardized reporting provides robust data for atmospheric models and, crucially, facilitates direct and meaningful comparison with the extensive  
210 body of literature on amine measurements.

**3.2. Inter-instrument Comparisons for Ammonia.** As presented in Figure 3a, the time-series data from the Vocus B and the Picarro G2103 CRDS analyzer demonstrate strong overall agreement during the campaign. Both instruments successfully track the same major pollution events and diurnal trends, establishing a baseline of reliability for the Vocus B in a real-world setting. However, a critical distinction is immediately apparent from the visual record. The data from the Vocus B (red) are  
215 characterized by sharp, high-magnitude peaks that capture rapid atmospheric fluctuations with high fidelity. In contrast, the data from the CRDS (grey), while tracking the same events, appear significantly dampened, consistently reporting lower concentrations during the most intense phases of the pollution plumes. This strong qualitative agreement is quantitatively confirmed by the linear regression analysis shown in Figure 3b. The robust correlation ( $R^2 = 0.76$ ,  $p < 0.01$ ) and near-unity slope (0.80) between the two time-aligned datasets indicate a lack of significant systematic bias and validate the overall  
220 accuracy of the Vocus B quantification. This excellent agreement across the entire concentration range lends high confidence to the Vocus B measurements. Consequently, the high-frequency peaks uniquely resolved by the Vocus B should be interpreted not as instrumental noise, but as genuine atmospheric features that the reference instrument was unable to fully capture.

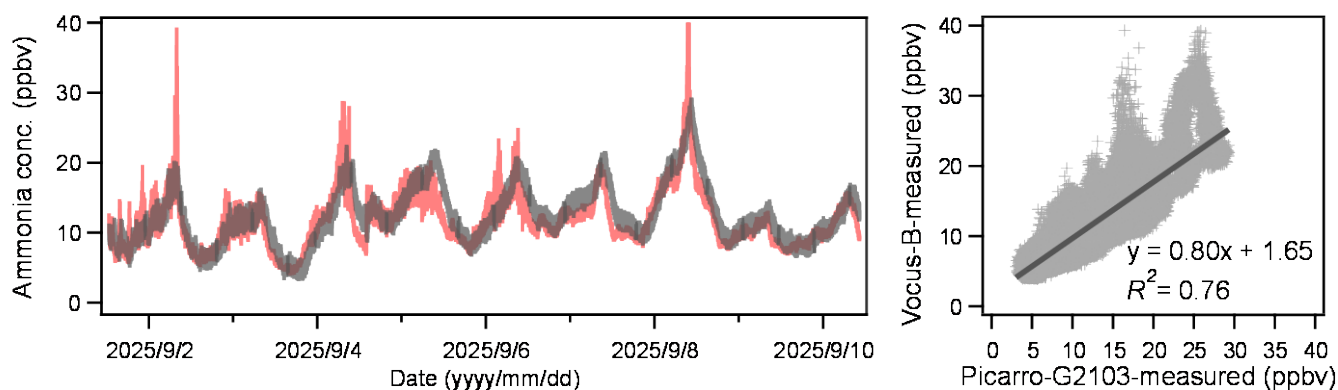


**Figure 3.** Inter-comparison of ambient ammonia measurements between the Vocus B (CIMS) and a co-located Picarro G2103  
225 (CRDS) analyzer. (a) Time series of  $\text{NH}_3$  concentrations (ppbv) from both instruments over a multi-day campaign in September 2025. (b) A linear regression scatter plot of the time-aligned datasets.

The discrepancy in resolving peak concentrations, despite both instruments reporting data at high frequency (0.5 Hz and 1 Hz respectively), stems from a fundamental difference in their effective temporal resolution. The Vocus B employs a direct-injection ion-molecule reactor with a gas residence time on the order of milliseconds, followed by near-instantaneous mass

230 analysis. This design allows it to function as a high-fidelity sensor, minimizing temporal averaging of the incoming air sample. Conversely, the CRDS achieves its high precision by making measurements within a physical optical cavity. The finite time required for complete gas exchange and mixing within this cell volume acts as an inherent physical averaging mechanism, effectively operating as a low-pass filter on the atmospheric signal and smoothing rapid concentration changes. For applications requiring accurate characterization of transient events, such as emission flux calculations from point sources, 235 industrial fence-line monitoring, or mobile source apportionment, the ability to resolve true peak concentrations is essential. A smoothed dataset can lead to potential underestimation of peak exposures and emission rates. The Vocus B, by faithfully capturing these dynamic features, provides a more accurate and actionable dataset for understanding and mitigating air pollution. Therefore, this inter-comparison establishes the Vocus B not merely as a validated instrument, but as a superior tool for investigating high-frequency atmospheric processes.

240 **3.3. Application 1: In-situ Atmospheric Measurement in Nanjing.** To demonstrate its capabilities for real-world atmospheric monitoring, the Vocus B was deployed for a multi-week, stationary in-situ campaign during winter in urban Nanjing. The detailed time series of simultaneously measured VOCs and VICs, presented in Figure 4a, reveals a highly complex and dynamic chemical environment characteristic of a megacity during the cold season. As expected for winter, the concentration of the biogenic tracer isoprene was consistently low (Guenther et al., 1995), often near the instrument's detection 245 limit. In contrast, anthropogenic VOCs like o-xylene and chlorobenzene exhibited highly variable concentrations, punctuated by frequent, sharp plumes that suggest the persistent influence of proximal industrial and traffic-related sources (Barletta et al., 2005). The simultaneous measurement of NH<sub>3</sub> provided another layer of crucial insight. While its average concentration was relatively low, consistent with reduced regional agricultural activity, its time series was far from static. It was characterized by frequent, sharp fluctuations that often decoupled from the industrial VOC plumes, strongly suggesting that non-agricultural 250 emissions-such as from traffic or industry-and potential regional transport events play a significant role in governing urban NH<sub>3</sub> levels during winter, a finding consistent with recent studies in other Chinese megacities (Chang et al., 2016; Chang et al., 2019).

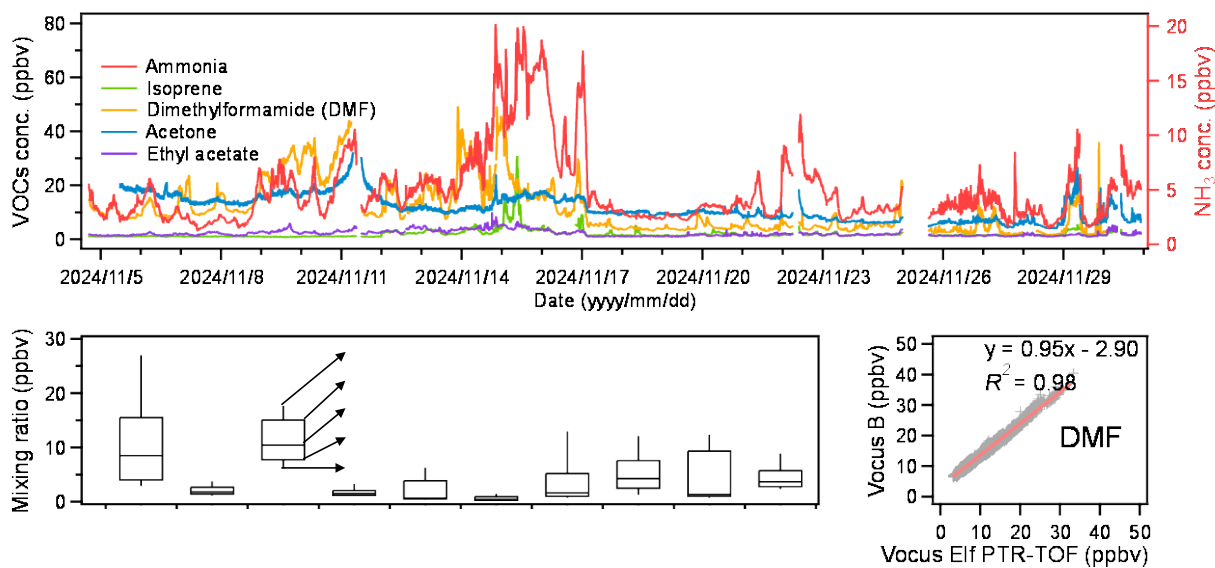


**Figure 4.** Simultaneous in-situ measurement of VOCs and VICs in urban Nanjing. (a) Time series of five representative VOCs and NH<sub>3</sub>. (b) Box-and-whisker plot summarizing the concentration distributions of key measured species. (c) A 1:1 scatter plot validating the high DMF measurements via an inter-comparison with a co-located Vocus Elf PTR-TOF.

A statistical overview of the key measured species, presented in the box-and-whisker plot in Figure 4b, encapsulates the wide dynamic range of the urban chemical environment captured by the Vocus B. The median concentrations of most pollutants were in the sub-ppbv to low single-ppbv range, levels which are broadly consistent with wintertime observations in other major urban centers in the Yangtze River Delta region (Zhu et al., 2018; Wang et al., 2020a; Liu et al., 2021). However, the upper quartiles and maxima (95<sup>th</sup> percentiles) extend significantly higher, confirming that the air quality at the site is frequently dominated by transient, high-concentration pollution events rather than a stable background. This statistical distribution highlights the necessity of high-time-resolution, multi-species measurements to accurately characterize exposure and atmospheric processes, particularly in highly-variable environments close to emission sources such as those found in urban and industrial areas. It was within this detailed analysis of the full dataset that an unexpected anomaly emerged: the concentrations of dimethylformamide (DMF) were not only highly variable but appeared to be extraordinarily high, a finding so unusual that it demanded rigorous, independent verification.

The most striking and environmentally significant result of the campaign was therefore the confirmation of these exceptionally high concentrations of DMF, an industrial solvent with significant health implications (Muzart, 2009; Ding and Jiao, 2012). The scatter plot in Figure 4c, which shows the inter-comparison between the Vocus B and a co-located, independent Vocus Elf PTR-TOF, provides that definitive validation. The near-perfect linear correlation ( $R^2 = 0.98$ ) between the two instruments confirms that the observed DMF plumes, often reaching tens of ppbv (Priestley et al., 2018), were a real and persistent feature of the local atmosphere. These concentrations are orders of magnitude higher than those typically reported in other urban areas,

275 which are usually in the low pptv to sub-ppbv range. Given that DMF is classified as a probable human carcinogen and a  
potent hepatotoxin (Gescher, 1993; Li and Zeng, 2019), its presence at these levels represents a potential and previously  
overlooked public health concern. The location of the measurement site within Nanjing R&D Park, a hub for advanced  
materials and chemical industries, provides a potential contextual clue. DMF is a widely used solvent in the production of  
polymers, synthetic leather, and pharmaceuticals (Wang and Lu, 2009), making a nearby industrial facility or a cluster of  
facilities within or near the park the plausible source of these emissions. This discovery showcases the immense value of the  
280 Vocus B not just as a monitoring tool, but as a powerful surveillance instrument for uncovering unknown local hotspots of  
hazardous air pollutants.

**3.4. Application 2: Mobile Laboratory Measurements along the Nanjing-Hefei Corridor.** To further validate the “all-in-  
one” capability of the Vocus B for mobile measurements, the instrument was deployed in a mobile laboratory for a transect  
along the approximately 170 km corridor connecting the urban fringes of Nanjing and Hefei. This region provided an ideal  
285 natural laboratory, encompassing a diverse landscape of suburban corridors, industrial zones, and a vast agricultural hinterland  
separating the two megacities. We selected two representative tracer species for this analysis: the VIC ammonia ( $\text{NH}_3$ ),  
detected as  $\text{C}_3\text{H}_{10}\text{NO}^+$  in the acetone mode, and the VOC styrene ( $\text{C}_8\text{H}_8$ ), detected as  $\text{C}_8\text{H}_8^+$  in the benzene mode. Ammonia is  
a well-established tracer for agricultural sources like livestock and fertilizer (Behera et al., 2013), while styrene is a strong  
indicator of industrial activity, primarily used in the production of polystyrene plastics and resins (Scheff and Wadden, 1993;  
290 Bond and Bolt, 1989). The ability to simultaneously measure these two distinct tracers from a single moving platform is the  
core strength demonstrated in this section, offering a unique method for pinpointing hidden emission sources.

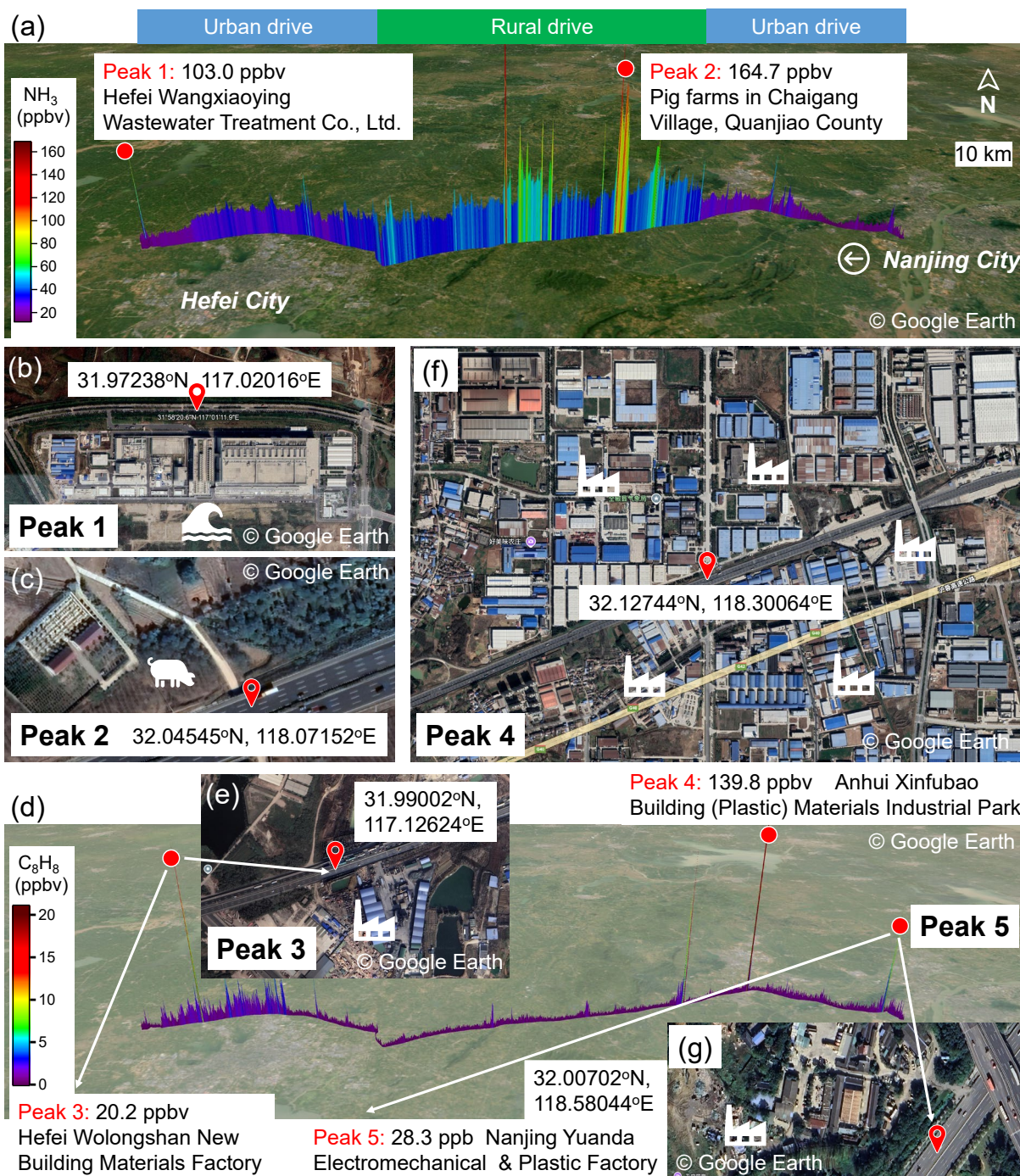


**Figure 5.** Simultaneous mobile measurements of NH<sub>3</sub> (a VIC) and styrene (a VOC) along the Nanjing-Hefei corridor. (a) 3D side-view of the NH<sub>3</sub> transect, showing high, diffuse concentrations in the central rural drive section. (b) Satellite view of Peak 1, a 103.0 ppbv NH<sub>3</sub> plume from the Hefei Wangxiaoying Wastewater Treatment Plant. (c) Satellite view of Peak 2, a 164.7

ppbv NH<sub>3</sub> plume from a pig farm. (d) 3D side-view of the styrene transect, showing a low baseline punctuated by sharp industrial plumes. (e) Satellite view of Peak 3 (20.2 ppbv styrene) from a building materials factory. (f) Satellite view of Peak 4 (139.8 ppbv styrene) from a large plastic materials industrial park. (g) Satellite view of Peak 5 (28.3 ppbv) from an electromechanical and plastic factory. Source of images: © Google Earth.

300 The spatial distributions of ammonia and styrene, visualized as 3D side-views in Figure 5a and 5d, revealed starkly different pollution topographies that clearly delineated the urban-rural divide. The average mixing ratio of NH<sub>3</sub> across the entire transect was 29.0 ppbv, a level comparable to other of China's agriculturally influenced regions in summer. Its landscape was dominated by a broad, elevated, and highly variable plateau throughout the central "rural drive" section, with much lower and more stable concentrations observed in the urban/suburban areas flanking the two cities. This continuous but fluctuating high  
305 background is the classic signature of diffuse area sources, consistent with widespread agricultural activity. In sharp contrast, the styrene transect was characterized by a consistently low background of only 0.8 ppbv on average, which was dramatically punctuated by a series of extremely sharp, narrow plumes. This pattern is indicative of localized, high-intensity industrial point sources. These contrasting profiles—one a rolling terrain of biogenic and agricultural emissions, the other a flat plain interrupted by industrial spires—vividly illustrate the instrument's capacity to simultaneously capture and characterize fundamentally  
310 different source types for chemically unrelated species.

By combining the high-resolution chemical data with concurrent GPS and satellite imagery, we performed a detailed, source-by-source investigation of these plumes, demonstrating that indeed, every peak tells a story. For ammonia, these stories emerged from both urban and rural settings. Even within the generally low-concentration "urban drive" section near Hefei, a prominent peak (Peak 1) was identified, reaching a maximum concentration of 103.0 ppbv. As shown in Figure 5b, this plume  
315 was traced directly to the fence line of the Hefei Wangxiaoying Wastewater Treatment Plant, a large-scale facility processing 0.3 Tg of wastewater daily. Such facilities are well-documented as significant urban point sources of ammonia due to the microbial decomposition of nitrogenous waste in aeration basins and sludge treatment processes. Further along the transect, in the central rural region, an even more intense ammonia plume (Peak 2) soared to 164.7 ppbv. Closer inspection (Figure 5c) revealed that this measurement was made directly downwind of a concentrated animal feeding operation (CAFO), specifically  
320 a large-scale pig farm in Chaigang Village, a classic and potent source of high ammonia emissions from animal waste.

The sharp industrial plumes of styrene were equally traceable, each telling a story of localized manufacturing activity. For instance, Peak 3 and Peak 5, reaching 20.2 ppb and 28.3 ppb respectively (Figure 5e, 5g), were both linked to individual sources: a new building materials factory in the Wolongshan area of Hefei and an electromechanical and plastic factory in Nanjing, respectively. Both facilities utilize plastic and resin-based components in their production, consistent with the  
325 observed styrene plumes. The most remarkable feature of the styrene transect was Peak 4, which reached an extremely high concentration of 139.8 ppbv, an order of magnitude higher than the other plumes. Satellite imagery (Figure 5f) revealed that this was not a single factory but corresponded to a large industrial cluster—the Anhui Xinfubao Building (Plastic) Materials

Industrial Park-which is densely packed with numerous plastic and building material manufacturing facilities. The mobile laboratory transected this industrial park, and the resulting broad, intense peak represents the combined, overlapping emissions from multiple co-located sources. This mobile deployment effectively demonstrates the unique advantages of the Vocus B as an “all-in-one” analytical solution for detailed source identification, providing an unparalleled level of detail for understanding local and regional air quality.

**3.5. Application 3: Real-Time Monitoring of AMC Outgassing in a Simulated Semiconductor Process.** As mentioned above, the outgassing of AMCs from FOUP surfaces poses a direct and significant threat to semiconductor yield. Even at pptv- levels, these contaminants can cause catastrophic defects: acidic gases corrode metal interconnects; alkaline species such as NH<sub>3</sub> induce T-topping and line-width broadening in chemically amplified photoresists, thereby compromising lithographic precision; and organic molecules can generate pinholes or reduce adhesion during thin-film deposition. The data from our simulated FOUP experiment (Figure 6a) provide a clear, real-time visualization of these contamination risks and highlight the instrument’s capacity to provide actionable process control data.

The experiment successfully captured the full dynamic sequence of a contamination and cleaning event. During the initial phase ( $t < 4$  min), the instrument measured the background concentrations in the N<sub>2</sub> stream, which were: NH<sub>3</sub>: 56.4 pptv, Toluene: 2.5 pptv, HF: 2341.3 pptv, HCl: 26035.6 pptv, and SO<sub>2</sub>: 0.0 pptv. Upon injection, the instrument detected an immediate increase in all target AMCs, with concentrations reaching tens of ppbv for species like NH<sub>3</sub> (44.1 ppbv) and HCl (49.7 ppbv), simulating a significant contamination event (Figure 6b). The subsequent continuous N<sub>2</sub> purge initiated a clear decay trend for all compounds. After more than 30 mins of purging, the contaminant levels were markedly reduced to: NH<sub>3</sub>: 12701.9 pptv, Toluene: 265.1 pptv, HF: 5236.4 pptv, HCl: 9598.9 pptv, and SO<sub>2</sub>: 354.2 pptv.

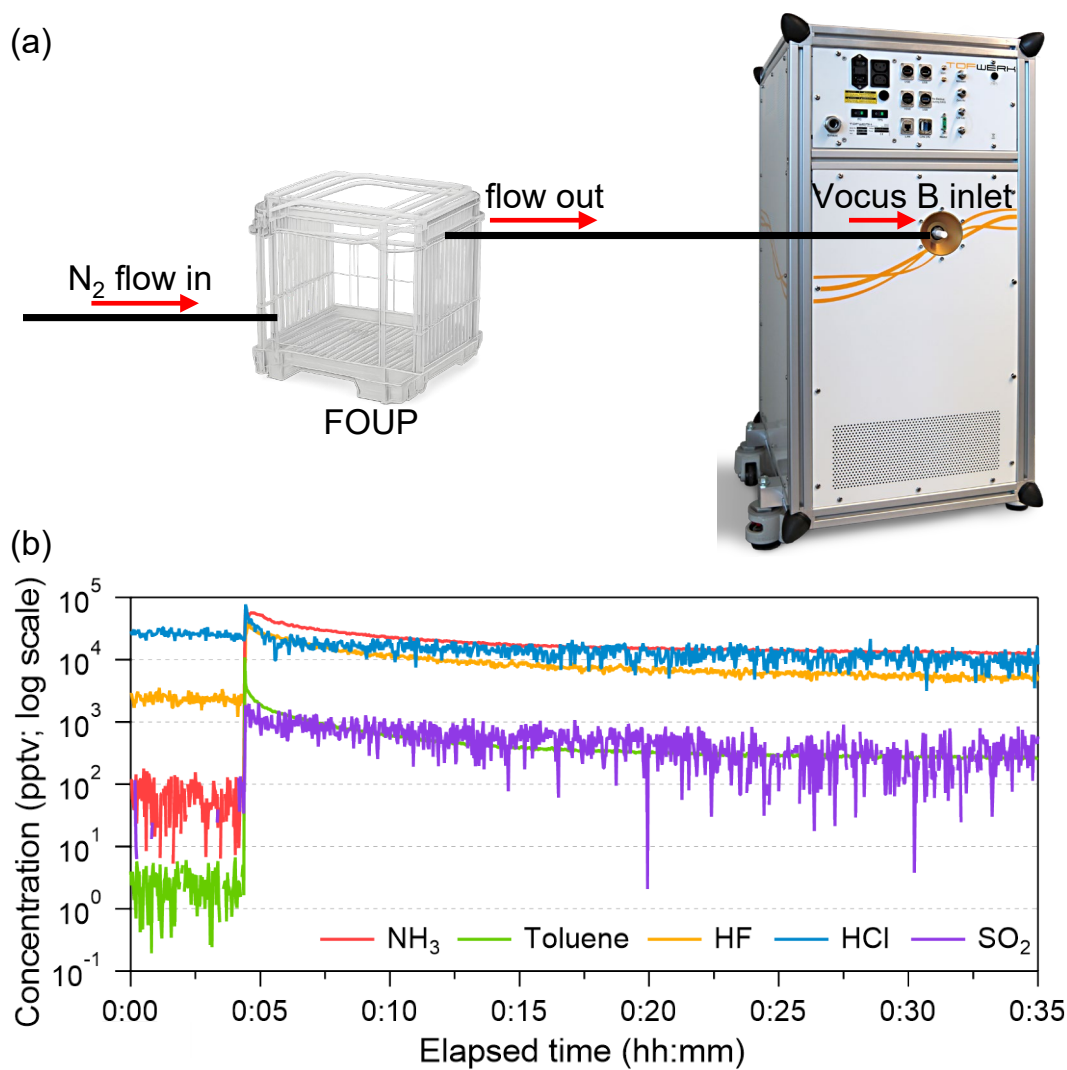


**Figure 6.** Real-time monitoring of Airborne Molecular Contaminant (AMC) outgassing in a simulated semiconductor process environment. (a) Schematic diagram of the experimental procedure, showing the high-purity nitrogen purge flow through the Front Opening Unified Pod (FOUP) and the direct, continuous sampling of the outgassed air by the Vocus B CI-TOF inlet. (b) Time-resolved concentration decay (logarithmic scale) of five key AMCs inside the FOUP following a simulated contamination event.

While some compounds were removed efficiently, the instrument's pptv-level sensitivity showed the prolonged persistence of the most problematic contaminants. Specifically, HCl and NH<sub>3</sub> exhibited much slower decay curves, suggesting strong, persistent interactions with the internal FOUP surfaces. This slow outgassing is a central industrial challenge; it means that cleaning processes that are not optimized for these specific compounds, or are not validated by sufficiently sensitive methods, can result in their persistent outgassing at levels capable of causing AMC problems and reducing wafer yield. This phenomenon

is often exacerbated by the *in-situ* formation of nm-sized salt particles (e.g., NH<sub>4</sub>Cl) from acid-base reactions, which evaporate very slowly and act as a long-term contamination reservoir.

360 This work demonstrates that the Vocus B provides the necessary real-time, quantitative feedback to manage these complex dynamics. Its ability to track the slow decay of problematic species down to the pptv-level ensures the true cleanliness of the FOUP can be verified. This allows for the data-driven optimization of cleaning cycles, the rapid qualification of new, low-outgassing FOUP materials, and provides a paradigm shift in a FAB operator's ability to mitigate AMC-related defects at their source.

#### 365 **4. Conclusions**

This study has provided a rigorous and comprehensive validation of the novel Vocus B CI-TOF-MS, establishing it as an “all-in-one” instrument for the simultaneous measurement of volatile organic and inorganic compounds. Our work confirms that the Vocus B demonstrates satisfied sensitivity and linearity for a wide range of pollutants and shows strong agreement with established analytical methods. It effectively addresses the long-standing analytical challenge of concurrently measuring VOCs and VICs. While specialized techniques like CRDS remain the gold standard for ultimate precision of individual species like NH<sub>3</sub>, the Vocus B offers a crucial advantage in versatility. By successfully integrating the measurement of organic and inorganic compounds into a single platform, it minimizes the logistical burden and synchronization errors associated with deploying multiple separate instruments. The instrument's success across three distinct and demanding applications—stationary urban monitoring, mobile source apportionment, and high-precision industrial process control—firmly establishes its role as a unified solution for multifaceted air quality challenges.

Looking forward, the true potential of this instrument lies in its application to these increasingly complex scientific and industrial challenges. The environmental datasets from this work provide a critical, high-resolution foundation for advanced regional pollution transport and source contribution models in a vital economic corridor. Its flexibility also opens new avenues for exploring emerging contaminants like amides and PFAS in future campaigns. Concurrently, its successful application to AMC monitoring is not merely a demonstration but a blueprint for proactive industrial process control. This enables a fundamental shift from reactive problem-solving to real-time quality assurance in semiconductor manufacturing, directly impacting device performance, reliability, and overall production efficiency. Future industrial applications will include the quality control of ultra-pure process gases and the optimization of abatement systems. In summary, the Vocus B CI-TOF-MS represents a significant advancement in analytical technology. It bridges the gap between environmental science and industrial quality control, offering a unified and powerful approach to deepen our understanding of complex chemical processes in the atmosphere and to provide actionable, real-time data for improving industrial processes and protecting human health.

## Data availability.

The data presented in this study are available upon reasonable request from the corresponding authors.

## Author contributions

390 YC: Conceptualization, Methodology, Investigation (Stationary and Mobile Campaigns), Formal Analysis, Writing – Original  
Draft, Writing – Review & Editing, Supervision, Project Administration. TD: Investigation (Stationary and Mobile  
Campaigns), Data Curation, Visualization. H.Y.: Investigation (Stationary Campaign), Resources. YY: Investigation (Mobile  
Campaign), Software. LZ: Investigation (FOUP Simulation), Resources. XL: Investigation (FOUP Simulation), Resources.  
WT: Conceptualization, Methodology, Writing – Review & Editing.

## 395 Acknowledgements.

YC thanks the National Key Research and Development Program of China (2023YFC3706202), the National Natural Science  
Foundation of China (Grant No. 41975166) and the Jiangsu Natural Science Fund for Excellent Young Scholars.

## Financial support.

This research has been financially supported by the National Key Research and Development Program of China  
400 (2023YFC3706202), the National Natural Science Foundation of China (Grant No. 41975166) and the Jiangsu Natural Science  
Fund for Excellent Young Scholars.

## References

- Almeida, J., Schobesberger, S., Kürten, A., Ortega, I. K., Kupiainen-Määttä, O., Praplan, A. P., Adamov, A., Amorim, A.,  
Bianchi, F., Breitenlechner, M., David, A., Dommen, J., Donahue, N. M., Downard, A., Dunne, E., Duplissy, J., Ehrhart, S.,  
405 Flagan, R. C., Franchin, A., Guida, R., Hakala, J., Hansel, A., Heinritzi, M., Henschel, H., Jokinen, T., Junninen, H., Kajos,  
M., Kangasluoma, J., Keskinen, H., Kupc, A., Kurtén, T., Kvashin, A. N., Laaksonen, A., Lehtipalo, K., Leiminger, M., Leppä,  
J., Loukonen, V., Makhmutov, V., Mathot, S., McGrath, M. J., Nieminen, T., Olenius, T., Onnela, A., Petäjä, T., Riccobono, F.,  
Riipinen, I., Rissanen, M., Rondo, L., Ruuskanen, T., Santos, F. D., Sarnela, N., Schallhart, S., Schnitzhofer, R., Seinfeld, J.  
H., Simon, M., Sipilä, M., Stozhkov, Y., Stratmann, F., Tomé, A., Tröstl, J., Tsagkogeorgas, G., Vaattovaara, P., Viisanen, Y.,  
410 Virtanen, A., Vrtala, A., Wagner, P. E., Weingartner, E., Wex, H., Williamson, C., Wimmer, D., Ye, P., Yli-Juuti, T., Carslaw,  
K. S., Kulmala, M., Curtius, J., Baltensperger, U., Worsnop, D. R., Vehkamäki, H., and Kirkby, J.: Molecular understanding  
of sulphuric acid–amine particle nucleation in the atmosphere, *Nature*, 502, 359–363, 10.1038/nature12663, 2013.  
Barletta, B., Meinardi, S., Sherwood Rowland, F., Chan, C.-Y., Wang, X., Zou, S., Yin Chan, L., and Blake, D. R.: Volatile  
organic compounds in 43 Chinese cities, *Atmospheric Environment*, 39, 5979–5990,  
415 <https://doi.org/10.1016/j.atmosenv.2005.06.029>, 2005.  
Behera, S. N., Sharma, M., Aneja, V. P., and Balasubramanian, R.: Ammonia in the atmosphere: a review on emission sources,  
atmospheric chemistry and deposition on terrestrial bodies, *Environmental Science and Pollution Research*, 20, 8092–8131,

- 10.1007/s11356-013-2051-9, 2013.
- 420 Bond, J. A. and Bolt, H. M.: Review of The Toxicology of Styrene, CRC Critical Reviews in Toxicology, 19, 227-249, 10.3109/10408448909037472, 1989.
- Chang, Y., Zou, Z., Deng, C., Huang, K., Collett, J. L., Lin, J., and Zhuang, G.: The importance of vehicle emissions as a source of atmospheric ammonia in the megacity of Shanghai, Atmos. Chem. Phys., 16, 3577-3594, 10.5194/acp-16-3577-2016, 2016.
- 425 Chang, Y., Zou, Z., Zhang, Y., Deng, C., Hu, J., Shi, Z., Dore, A. J., and Collett, J. L., Jr.: Assessing Contributions of Agricultural and Nonagricultural Emissions to Atmospheric Ammonia in a Chinese Megacity, Environmental Science & Technology, 53, 1822-1833, 10.1021/acs.est.8b05984, 2019.
- Chang, Y., Gao, Y., Lu, Y., Qiao, L., Kuang, Y., Cheng, K., Wu, Y., Lou, S., Jing, S., Wang, H., and Huang, C.: Discovery of a Potent Source of Gaseous Amines in Urban China, Environmental Science & Technology Letters, 8, 725-731, 10.1021/acs.estlett.1c00229, 2021.
- 430 Chang, Y., Wang, H., Gao, Y., Jing, S. a., Lu, Y., Lou, S., Kuang, Y., Cheng, K., Ling, Q., Zhu, L., Tan, W., and Huang, R.-J.: Nonagricultural Emissions Dominate Urban Atmospheric Amines as Revealed by Mobile Measurements, Geophysical Research Letters, 49, e2021GL097640, <https://doi.org/10.1029/2021GL097640>, 2022.
- Chen, R., Shiue, A., Liu, J., Zhi, Y., Zhang, D., Xia, F., and Leggett, G.: Integrated on-site collection and off-site analysis of airborne molecular contamination in cleanrooms for integrated circuit manufacturing processes, Building and Environment, 435, 214, 108941, <https://doi.org/10.1016/j.buildenv.2022.108941>, 2022.
- de Gouw, J. and Warneke, C.: Measurements of volatile organic compounds in the earth's atmosphere using proton-transfer-reaction mass spectrometry, Mass Spectrometry Reviews, 26, 223-257, <https://doi.org/10.1002/mas.20119>, 2007.
- Den, W., Bai, H., and Kang, Y.: Organic Airborne Molecular Contamination in Semiconductor Fabrication Clean Rooms: A Review, Journal of The Electrochemical Society, 153, G149, 10.1149/1.2147286, 2006.
- 440 Den, W., Hu, S.-C., Garza, C. M., and Ali Zargar, O.: Review—Airborne Molecular Contamination: Recent Developments in the Understanding and Minimization for Advanced Semiconductor Device Manufacturing, ECS Journal of Solid State Science and Technology, 9, 064003, 10.1149/2162-8777/aba080, 2020.
- Ding, S. and Jiao, N.: N,N-Dimethylformamide: A Multipurpose Building Block, Angewandte Chemie International Edition, 51, 9226-9237, <https://doi.org/10.1002/anie.201200859>, 2012.
- 445 Ehn, M., Thornton, J. A., Kleist, E., Sipilä, M., Junninen, H., Pullinen, I., Springer, M., Rubach, F., Tillmann, R., Lee, B., Lopez-Hilfiker, F., Andres, S., Acir, I.-H., Rissanen, M., Jokinen, T., Schobesberger, S., Kangasluoma, J., Kontkanen, J., Nieminen, T., Kurtén, T., Nielsen, L. B., Jørgensen, S., Kjaergaard, H. G., Canagaratna, M., Maso, M. D., Berndt, T., Petäjä, T., Wahner, A., Kerminen, V.-M., Kulmala, M., Worsnop, D. R., Wildt, J., and Mentel, T. F.: A large source of low-volatility secondary organic aerosol, Nature, 506, 476-479, 10.1038/nature13032, 2014.
- 450 Gescher, A.: Metabolism of N,N-dimethylformamide: Key to the understanding of its toxicity, Chemical Research in Toxicology, 6, 245-251, 10.1021/tx00033a001, 1993.
- Gu, B., Zhang, L., Van Dingenen, R., Vieno, M., Van Grinsven, H. J. M., Zhang, X., Zhang, S., Chen, Y., Wang, S., Ren, C., Rao, S., Holland, M., Winiwarter, W., Chen, D., Xu, J., and Sutton, M. A.: Abating ammonia is more cost-effective than nitrogen oxides for mitigating PM<sub>2.5</sub> air pollution, Science, 374, 758-762, 10.1126/science.abf8623, 2021.
- 455 Gu, M., Pan, Y., Walters, W. W., Sun, Q., Song, L., Wang, Y., Xue, Y., and Fang, Y.: Vehicular Emissions Enhanced Ammonia Concentrations in Winter Mornings: Insights from Diurnal Nitrogen Isotopic Signatures, Environmental Science & Technology, 56, 1578-1585, 10.1021/acs.est.1c05884, 2022.
- Guenther, A., Hewitt, C. N., Erickson, D., Fall, R., Geron, C., Graedel, T., Harley, P., Klinger, L., Lerdau, M., McKay, W. A., Pierce, T., Scholes, B., Steinbrecher, R., Tallamraju, R., Taylor, J., and Zimmerman, P.: A global model of natural volatile organic compound emissions, Journal of Geophysical Research: Atmospheres, 100, 8873-8892, <https://doi.org/10.1029/94JD02950>, 1995.
- 460 Hanson, D. R., McMurry, P. H., Jiang, J., Tanner, D., and Huey, L. G.: Ambient Pressure Proton Transfer Mass Spectrometry: Detection of Amines and Ammonia, Environmental Science & Technology, 45, 8881-8888, 10.1021/es201819a, 2011.
- Huang, G., Hou, J., and Zhou, X.: A Measurement Method for Atmospheric Ammonia and Primary Amines Based on Aqueous Sampling, OPA Derivatization and HPLC Analysis, Environmental Science & Technology, 43, 5851-5856, 10.1021/es900988q, 2009.
- Isaacman, G., Kreisberg, N. M., Worton, D. R., Hering, S. V., and Goldstein, A. H.: A versatile and reproducible automatic

- injection system for liquid standard introduction: application to in-situ calibration, *Atmos. Meas. Tech.*, 4, 1937-1942, 10.5194/amt-4-1937-2011, 2011.
- 470 Kirkby, J., Curtius, J., Almeida, J., Dunne, E., Duplissy, J., Ehrhart, S., Franchin, A., Gagné, S., Ickes, L., Kürten, A., Kupc, A., Metzger, A., Riccobono, F., Rondo, L., Schobesberger, S., Tsagkogeorgas, G., Wimmer, D., Amorim, A., Bianchi, F., Breitenlechner, M., David, A., Dommen, J., Downard, A., Ehn, M., Flagan, R. C., Haider, S., Hansel, A., Hauser, D., Jud, W., Junninen, H., Kreissl, F., Kvashin, A., Laaksonen, A., Lehtipalo, K., Lima, J., Lovejoy, E. R., Makhmutov, V., Mathot, S., Mikkilä, J., Minginette, P., Mogo, S., Nieminen, T., Onnela, A., Pereira, P., Petäjä, T., Schnitzhofer, R., Seinfeld, J. H., Sipilä, M., Stozhkov, Y., Stratmann, F., Tomé, A., Vanhanen, J., Viisanen, Y., Vrtala, A., Wagner, P. E., Walther, H., Weingartner, E., 475 Wex, H., Winkler, P. M., Carslaw, K. S., Worsnop, D. R., Baltensperger, U., and Kulmala, M.: Role of sulphuric acid, ammonia and galactic cosmic rays in atmospheric aerosol nucleation, *Nature*, 476, 429-433, 10.1038/nature10343, 2011.
- Lee, B. H., Lopez-Hilfiker, F. D., Mohr, C., Kurtén, T., Worsnop, D. R., and Thornton, J. A.: An Iodide-Adduct High-Resolution Time-of-Flight Chemical-Ionization Mass Spectrometer: Application to Atmospheric Inorganic and Organic Compounds, 480 *Environmental Science & Technology*, 48, 6309-6317, 10.1021/es500362a, 2014.
- Li, M.-J. and Zeng, T.: The deleterious effects of N,N-dimethylformamide on liver: A mini-review, *Chemico-Biological Interactions*, 298, 129-136, <https://doi.org/10.1016/j.cbi.2018.12.011>, 2019.
- Link, M. F., Claffin, M. S., Cecelski, C. E., Akande, A. A., Kilgour, D., Heine, P. A., Coggon, M., Stockwell, C. E., Jensen, A., Yu, J., Huynh, H. N., Ditto, J. C., Warneke, C., Dresser, W., Gemmell, K., Jorga, S., Robertson, R. L., de Gouw, J., Bertram, 485 T., Abbatt, J. P. D., Borduas-Dedekind, N., and Poppendieck, D.: Product ion distributions using  $\text{H}_3\text{O}^+$  proton-transfer-reaction time-of-flight mass spectrometry (PTR-ToF-MS): mechanisms, transmission effects, and instrument-to-instrument variability, *Atmos. Meas. Tech.*, 18, 1013-1038, 10.5194/amt-18-1013-2025, 2025.
- Liu, Y., Wang, H., Jing, S., Peng, Y., Gao, Y., Yan, R., Wang, Q., Lou, S., Cheng, T., and Huang, C.: Strong regional transport of volatile organic compounds (VOCs) during wintertime in Shanghai megacity of China, *Atmospheric Environment*, 244, 490 117940, <https://doi.org/10.1016/j.atmosenv.2020.117940>, 2021.
- Mansouri, M., Koval, P., Sharifzadeh, S., and Sánchez-Portal, D.: Molecular Doping in the Organic Semiconductor Diindenoperylene: Insights from Many-Body Perturbation Theory, *J Phys Chem C Nanomater Interfaces*, 127, 16668-16678, 10.1021/acs.jpcc.3c03758, 2023.
- McDonald Brian, C., de Gouw Joost, A., Gilman Jessica, B., Jathar Shantanu, H., Akherati, A., Cappa Christopher, D., Jimenez 495 Jose, L., Lee-Taylor, J., Hayes Patrick, L., McKeen Stuart, A., Cui Yu, Y., Kim, S.-W., Gentner Drew, R., Isaacman-VanWertz, G., Goldstein Allen, H., Harley Robert, A., Frost Gregory, J., Roberts James, M., Ryerson Thomas, B., and Trainer, M.: Volatile chemical products emerging as largest petrochemical source of urban organic emissions, *Science*, 359, 760-764, 10.1126/science.aaq0524, 2018.
- Mohr, C., Thornton, J. A., Heitto, A., Lopez-Hilfiker, F. D., Lutz, A., Riipinen, I., Hong, J., Donahue, N. M., Hallquist, M., 500 Petäjä, T., Kulmala, M., and Yli-Juuti, T.: Molecular identification of organic vapors driving atmospheric nanoparticle growth, *Nature communications*, 10, 4442, 10.1038/s41467-019-12473-2, 2019.
- Murphy, S. M., Sorooshian, A., Kroll, J. H., Ng, N. L., Chhabra, P., Tong, C., Surratt, J. D., Knipping, E., Flagan, R. C., and Seinfeld, J. H.: Secondary aerosol formation from atmospheric reactions of aliphatic amines, *Atmos. Chem. Phys.*, 7, 2313-2337, 10.5194/acp-7-2313-2007, 2007.
- 505 Muzart, J.: N,N-Dimethylformamide: much more than a solvent, *Tetrahedron*, 65, 8313-8323, <https://doi.org/10.1016/j.tet.2009.06.091>, 2009.
- Nie, W., Yan, C., Huang, D. D., Wang, Z., Liu, Y., Qiao, X., Guo, Y., Tian, L., Zheng, P., Xu, Z., Li, Y., Xu, Z., Qi, X., Sun, P., Wang, J., Zheng, F., Li, X., Yin, R., Dallenbach, K. R., Bianchi, F., Petäjä, T., Zhang, Y., Wang, M., Schervish, M., Wang, S., Qiao, L., Wang, Q., Zhou, M., Wang, H., Yu, C., Yao, D., Guo, H., Ye, P., Lee, S., Li, Y. J., Liu, Y., Chi, X., Kerminen, V.-M., 510 Ehn, M., Donahue, N. M., Wang, T., Huang, C., Kulmala, M., Worsnop, D., Jiang, J., and Ding, A.: Secondary organic aerosol formed by condensing anthropogenic vapours over China's megacities, *Nat Geosci*, 15, 255-261, 10.1038/s41561-022-00922-5, 2022.
- Norman, M., Hansel, A., and Wisthaler, A.:  $\text{O}_2^+$  as reagent ion in the PTR-MS instrument: Detection of gas-phase ammonia, *International Journal of Mass Spectrometry*, 265, 382-387, <https://doi.org/10.1016/j.ijms.2007.06.010>, 2007.
- 515 Park, J. H., Goldstein, A. H., Timkovsky, J., Fares, S., Weber, R., Karlik, J., and Holzinger, R.: Active Atmosphere-Ecosystem Exchange of the Vast Majority of Detected Volatile Organic Compounds, *Science*, 341, 643-647, 10.1126/science.1235053, 2013.

- Pfeifer, J., Simon, M., Heinritzi, M., Piel, F., Weitz, L., Wang, D., Granzin, M., Müller, T., Bräkling, S., Kirkby, J., Curtius, J., and Kürten, A.: Measurement of ammonia, amines and iodine compounds using protonated water cluster chemical ionization mass spectrometry, *Atmos. Meas. Tech.*, 13, 2501-2522, 10.5194/amt-13-2501-2020, 2020.
- Place, B. K., Quilty, A. T., Di Lorenzo, R. A., Ziegler, S. E., and VandenBoer, T. C.: Quantitation of 11 alkylamines in atmospheric samples: separating structural isomers by ion chromatography, *Atmos. Meas. Tech.*, 10, 1061-1078, 10.5194/amt-10-1061-2017, 2017.
- Priestley, M., Le Breton, M., Bannan, T. J., Leather, K. E., Bacak, A., Reyes-Villegas, E., De Vocht, F., Shallcross, B. M. A., Brazier, T., Anwar Khan, M., Allan, J., Shallcross, D. E., Coe, H., and Percival, C. J.: Observations of Isocyanate, Amide, Nitrate, and Nitro Compounds From an Anthropogenic Biomass Burning Event Using a ToF-CIMS, *Journal of Geophysical Research: Atmospheres*, 123, 7687-7704, <https://doi.org/10.1002/2017JD027316>, 2018.
- Pye, H. O. T., D'Ambro, E. L., Lee, B. H., Schobesberger, S., Takeuchi, M., Zhao, Y., Lopez-Hilfiker, F., Liu, J., Shilling, J. E., Xing, J., Mathur, R., Middlebrook, A. M., Liao, J., Welti, A., Graus, M., Warneke, C., de Gouw, J. A., Holloway, J. S., Ryerson, T. B., Pollack, I. B., and Thornton, J. A.: Anthropogenic enhancements to production of highly oxygenated molecules from autoxidation, *Proceedings of the National Academy of Sciences*, 116, 6641-6646, 10.1073/pnas.1810774116, 2019.
- Reinecke, T., Leiminger, M., Jordan, A., Wisthaler, A., and Müller, M.: Ultrahigh Sensitivity PTR-MS Instrument with a Well-Defined Ion Chemistry, *Anal Chem*, 95, 11879-11884, 10.1021/acs.analchem.3c02669, 2023.
- Riva, M., Pospisilova, V., Frege, C., Perrier, S., Bansal, P., Jorga, S., Sturm, P., Thornton, J. A., Rohner, U., and Lopez-Hilfiker, F.: Evaluation of a reduced-pressure chemical ion reactor utilizing adduct ionization for the detection of gaseous organic and inorganic species, *Atmos. Meas. Tech.*, 17, 5887-5901, 10.5194/amt-17-5887-2024, 2024.
- Scheff, P. A. and Wadden, R. A.: Receptor modeling of volatile organic compounds. 1. Emission inventory and validation, *Environmental Science & Technology*, 27, 617-625, 10.1021/es00041a005, 1993.
- Seinfeld and Pandis, S. N.: *Atmospheric chemistry and physics: From air pollution to climate change*, John Wiley & Sons 2012.
- Sullivan, A. P., Benedict, K. B., Carrico, C. M., Dubey, M. K., Schichtel, B. A., and Collett, J. L.: A Quantitative Method to Measure and Speciate Amines in Ambient Aerosol Samples, *Atmosphere*, 11, 808, 2020.
- Tiszenkel, L., Flynn, J. H., and Lee, S. H.: Measurement report: Urban ammonia and amines in Houston, Texas, *Atmos. Chem. Phys.*, 24, 11351-11363, 10.5194/acp-24-11351-2024, 2024.
- Van Damme, M., Clarisse, L., Whitburn, S., Hadji-Lazaro, J., Hurtmans, D., Clerbaux, C., and Coheur, P.-F.: Industrial and agricultural ammonia point sources exposed, *Nature*, 564, 99-103, 10.1038/s41586-018-0747-1, 2018.
- VandenBoer, T. C., Petroff, A., Markovic, M. Z., and Murphy, J. G.: Size distribution of alkyl amines in continental particulate matter and their online detection in the gas and particle phase, *Atmos. Chem. Phys.*, 11, 4319-4332, 10.5194/acp-11-4319-2011, 2011.
- Vera, T., Villanueva, F., Wimmerová, L., and Tolis, E. I.: An overview of methodologies for the determination of volatile organic compounds in indoor air, *Applied Spectroscopy Reviews*, 57, 625-674, 10.1080/05704928.2022.2085735, 2022.
- Wang, M., Qin, W., Chen, W., Zhang, L., Zhang, Y., Zhang, X., and Xie, X.: Seasonal variability of VOCs in Nanjing, Yangtze River delta: Implications for emission sources and photochemistry, *Atmospheric Environment*, 223, 117254, <https://doi.org/10.1016/j.atmosenv.2019.117254>, 2020a.
- Wang, M., Kong, W., Marten, R., He, X.-C., Chen, D., Pfeifer, J., Heitto, A., Kontkanen, J., Dada, L., Kürten, A., Yli-Juuti, T., Manninen, H. E., Amanatidis, S., Amorim, A., Baalbaki, R., Baccarini, A., Bell, D. M., Bertozzi, B., Bräkling, S., Brilke, S., Murillo, L. C., Chiu, R., Chu, B., De Menezes, L.-P., Duplissy, J., Finkenzeller, H., Carracedo, L. G., Granzin, M., Guida, R., Hansel, A., Hofbauer, V., Krechmer, J., Lehtipalo, K., Lamkaddam, H., Lampimäki, M., Lee, C. P., Makhmutov, V., Marie, G., Mathot, S., Mauldin, R. L., Mentler, B., Müller, T., Onnela, A., Partoll, E., Petäjä, T., Philippov, M., Pospisilova, V., Ranjithkumar, A., Rissanen, M., Rörup, B., Scholz, W., Shen, J., Simon, M., Sipilä, M., Steiner, G., Stolzenburg, D., Tham, Y. J., Tomé, A., Wagner, A. C., Wang, D. S., Wang, Y., Weber, S. K., Winkler, P. M., Wlasits, P. J., Wu, Y., Xiao, M., Ye, Q., Zauner-Wieczorek, M., Zhou, X., Volkamer, R., Riipinen, I., Dommen, J., Curtius, J., Baltensperger, U., Kulmala, M., Worsnop, D. R., Kirkby, J., Seinfeld, J. H., El-Haddad, I., Flagan, R. C., and Donahue, N. M.: Rapid growth of new atmospheric particles by nitric acid and ammonia condensation, *Nature*, 581, 184-189, 10.1038/s41586-020-2270-4, 2020b.
- Wang, V.-S. and Lu, M.-Y.: Application of solid-phase microextraction and gas chromatography-mass spectrometry for measuring chemicals in saliva of synthetic leather workers, *Journal of Chromatography B*, 877, 24-32, <https://doi.org/10.1016/j.jchromb.2008.11.006>, 2009.
- Yan, F., Chen, W., Wang, X., Jia, S., Mao, J., Cao, J., and Chang, M.: Significant Increase in Ammonia Emissions in China:

- Considering Nonagricultural Sectors Based on Isotopic Source Apportionment, *Environmental Science & Technology*, 58, 2423-2433, 10.1021/acs.est.3c07222, 2024.
- 570 Yang, D., Zhu, S., Ma, Y., Zhou, L., Zheng, F., Wang, L., Jiang, J., and Zheng, J.: Emissions of Ammonia and Other Nitrogen-Containing Volatile Organic Compounds from Motor Vehicles under Low-Speed Driving Conditions, *Environmental Science & Technology*, 56, 5440-5447, 10.1021/acs.est.2c00555, 2022.
- 575 Yao, L., Wang, M. Y., Wang, X. K., Liu, Y. J., Chen, H. F., Zheng, J., Nie, W., Ding, A. J., Geng, F. H., Wang, D. F., Chen, J. M., Worsnop, D. R., and Wang, L.: Detection of atmospheric gaseous amines and amides by a high-resolution time-of-flight chemical ionization mass spectrometer with protonated ethanol reagent ions, *Atmos. Chem. Phys.*, 16, 14527-14543, 10.5194/acp-16-14527-2016, 2016.
- 580 Yao, L., Garmash, O., Bianchi, F., Zheng, J., Yan, C., Kontkanen, J., Junninen, H., Mazon, S. B., Ehn, M., Paasonen, P., Sipilä, M., Wang, M., Wang, X., Xiao, S., Chen, H., Lu, Y., Zhang, B., Wang, D., Fu, Q., Geng, F., Li, L., Wang, H., Qiao, L., Yang, X., Chen, J., Kerminen, V.-M., Petäjä, T., Worsnop, D. R., Kulmala, M., and Wang, L.: Atmospheric new particle formation from sulfuric acid and amines in a Chinese megacity, *Science*, 361, 278-281, doi:10.1126/science.aao4839, 2018.
- 585 You, Y., Kanawade, V. P., de Gouw, J. A., Guenther, A. B., Madronich, S., Sierra-Hernández, M. R., Lawler, M., Smith, J. N., Takahama, S., Ruggeri, G., Koss, A., Olson, K., Baumann, K., Weber, R. J., Nenes, A., Guo, H., Edgerton, E. S., Porcelli, L., Brune, W. H., Goldstein, A. H., and Lee, S. H.: Atmospheric amines and ammonia measured with a chemical ionization mass spectrometer (CIMS), *Atmos. Chem. Phys.*, 14, 12181-12194, 10.5194/acp-14-12181-2014, 2014.
- 590 Yuan, B., Koss, A. R., Warneke, C., Coggon, M., Sekimoto, K., and de Gouw, J. A.: Proton-Transfer-Reaction Mass Spectrometry: Applications in Atmospheric Sciences, *Chemical reviews*, 117, 13187-13229, 10.1021/acs.chemrev.7b00325, 2017a.
- 595 Yuan, B., Coggon, M. M., Koss, A. R., Warneke, C., Eilerman, S., Peischl, J., Aikin, K. C., Ryerson, T. B., and de Gouw, J. A.: Emissions of volatile organic compounds (VOCs) from concentrated animal feeding operations (CAFOs): chemical compositions and separation of sources, *Atmos. Chem. Phys.*, 17, 4945-4956, 10.5194/acp-17-4945-2017, 2017b.
- Zhang, Y., Wang, L., Sun, T., and Huang, B.: Vehicle-based monitoring and AI unravel patterns of on-road carbon and pollutant emissions, *The Innovation Geoscience*, 2, 100085, 10.59717/j.xinn-geo.2024.100085, 2024.
- Zheng, J., Ma, Y., Chen, M., Zhang, Q., Wang, L., Khalizov, A. F., Yao, L., Wang, Z., Wang, X., and Chen, L.: Measurement of atmospheric amines and ammonia using the high resolution time-of-flight chemical ionization mass spectrometry, *Atmospheric Environment*, 102, 249-259, <https://doi.org/10.1016/j.atmosenv.2014.12.002>, 2015.
- Zhu, H., Wang, H., Jing, S., Wang, Y., Cheng, T., Tao, S., Lou, S., Qiao, L., Li, L., and Chen, J.: Characteristics and sources of atmospheric volatile organic compounds (VOCs) along the mid-lower Yangtze River in China, *Atmospheric Environment*, 190, 232-240, <https://doi.org/10.1016/j.atmosenv.2018.07.026>, 2018.